Journal of Computers Vol. 32 No. 6, 2021, pp. 227-238
doi:10.53106/199115992021123206020

Influence of Inner Surface Reflection Characteristics on Inflatable Sphere Temperature in Space

Fu-Bing Li[1*], Jun-Min Leng[1], Xiao-Jian Xu[2]

[1] School of Information & Communication Engineering, Beijing Information Science & Technology University, Beijing 100101, ROC
{lifubing, lengjunmin}@bistu.edu.cn

[2] School of Electronics and Information Engineering, Beihang University, Beijing 100191, ROC
xiaojianxu@buaa.edu.cn

Received 1 October 2021; Revised 25 November 2021; Accepted 5 December 2021

Abstract. The differential equation of heat transfer for a space point target is established, and the theoretical temperature change of the point target is herein calculated. Then, for the inflatable sphere in space with specularly-reflecting or diffusely-reflecting inner surface, by considering the multi-layer ultra-thin materials as equivalent to a single-layer material, the unsteady heat transfer equation of micro-facets is established for calculating the superficial temperature distribution of the sphere and inducing its equivalent radiation temperature. The calculation results show that the equivalent radiation temperature of the target is consistent with the theoretical temperature change of the point target. The specular or diffuse reflection characteristics of inner surfaces do not affect the equivalent radiation temperature of the target. Influenced by the radiation transfer coefficient, the superficial temperature difference of the sphere with specularly-reflecting inner surface is larger than that with diffusely-reflecting inner surface, and the lower the emissivity, the more obvious it is. When the emissivity is close to 1, the superficial temperature distribution in both cases tends to be consistent.

Keywords: specular reflection, diffuse reflection, inner surface, temperature, sphere

1 Introduction

1.1 Background and Related Work

Temperature and infrared characteristics of the space objects are important basis for target tracking and identification [1-5], especially for space non-cooperative targets [6-7]. Spatial inflatable decoys are one of the commonly used penetration methods for space non-cooperative objects. As the inflatable decoys are very light, it is convenient for ballistic missiles to carry [8-9]. The decoy can be designed in a variety of forms such as sphere and cone. During the midcourse trajectory, a large number of decoys can be released to form a decoy cloud, making it difficult to distinguish the true target among the decoys and thus reducing the valuable defense time [10-11].

As spatial inflatable decoys can effectively reduce the detection probability of mid-course targets and increase the difficulty of target recognition. Scholars have done vast research on the temperature and infrared characteristics of space objects. Sessler et al. regarded inflatable spheres as point targets and studied the influence of coating materials on temperature in detail [12]. Heat transfer equation of the space object is given and the steady-state equivalent radiation temperature with different coatings are derived. In addition, the transient temperature curve as a function of time is also displayed. As the object is regarded as a point target, only the equivalent radiation temperature of the object is calculated. Although the surface temperature distribution of the target is important, it is not included in their studies. Yang et al. studied the temperature and infrared radiation of the spatial balloons with and without object

* Corresponding Author

inside the balloon [13]. Balloons were assumed to be gray and rotating along the spinning axis. Results indicate that both the temperature and infrared signal are similar in such circumstance. Liu et al. calculated the heat transfer coefficient of the envelope target (i.e., an inflatable balloon with an object inside) with different reflecting characteristics [14]. The inner surface of the balloon is specularly-reflecting while the outside of the object inside the balloon is diffusely-reflecting. In such case, heat transfer coefficient should be used to calculate the radiation heat transfer instead of angle factor usually used in gray system. Shen et al. calculated the temperature and infrared radiation of a two-layer sphere-cone warhead. For comparison, a sphere-cone balloon was also introduced into the calculation [15]. Yang et al. studied the warhead envelop ball's temperature variation in space with and without solar radiation. The ball was composed of three ultra-thin materials which are aluminum, polyester and aluminum films from the inside out. The equivalent radiation temperature of the envelop ball was calculated under the circumstances with and without solar radiation. For comparison, the temperature of an empty ball was also computed [16]. Fang et al. analyzed the infrared radiation of the two-layer material inflatable sphere with different coatings. [17].

1.2 Problem Statement and Motivation

There are two main problems in the current research on space balloon targets or envelope targets. First, most research focused on the equivalent radiation temperature of the space object and ignored the surface temperature distribution. For an inflatable sphere in space, the strong solar radiation may produce a large temperature difference on the target surface. Only using the point target temperature for calculation will cause a big error in some observation orientations. So it is necessary to study the surface temperature distribution of the object. The temperature difference on the inflatable sphere will enhance the radiation heat transfer between its inner superficial parts, and the reflective characteristics of the inner surface (specular reflection, diffuse reflection, etc.) will affect the distribution of radiation energy in different areas, and further affect the temperature distribution of the target.

Second, most of the existing research does not describe much on the radiative heat transfer inside the balloon. Even if it involves radiation heat transfer, inner surface of the object is usually assumed to be diffusely-reflecting and the Gebhart method is applied to iteratively calculate radiation heat transfer only by using the angle factor. Zhang et al. provided a method to solve the radiation transfer coefficient between gray body facets by using the angle coefficient [18], which can permit us to avoid applying the iterative process and speed up the calculation. However, a reference [12] pointed out that the coating on the inner surface of the inflatable sphere may be very smooth, and the inner surface will have good specular reflection other than diffuse reflection. In this case, it is necessary to use the radiation transfer coefficient to calculate the radiative heat transfer inside the balloon, and then the accuracy of calculated temperature distribution can be improved.

1.3 Innovation

In this paper, the equivalent model of ultra-thin multilayer material is used to study the target temperature distribution on the specularly-reflecting inner surface and its similarities with and differences from the target temperature distribution on the diffusely-reflecting inner surface. The innovation of the thesis is to find the influence of different inner surface characteristics on the target surface temperature distribution. Compared with diffusely-reflecting inner surface, the specularly-reflecting inner surface on the temperature distribution of the target surface is not particularly significant, especially when the reflectivity is less than 0.5. Therefore, when the temperature calculation accuracy is not particularly high, diffusely-reflecting inner surface can be used instead of specularly-reflecting inner surface to calculate radiative heat transfer. In particular, for a spherical target, since the radiation transfer coefficient of the diffusely-reflecting inner surface is equal to its angular coefficient, the time for the Monte Carlo method to calculate the radiation transfer coefficient can be greatly saved.

2 Equivalent Model of Ultra-Thin Multilayer Media

It can be known from the literature [12] that the wall thickness of the spatial inflatable sphere composed of multi-layer ultrathin materials is extremely thin (< 0.1mm), so it is reasonable to assume that the

inflatable sphere temperature is the same along the thickness direction, and the multi-layer ultrathin media can be taken as equivalent to a single-layer material [19], as shown in Fig. 1.

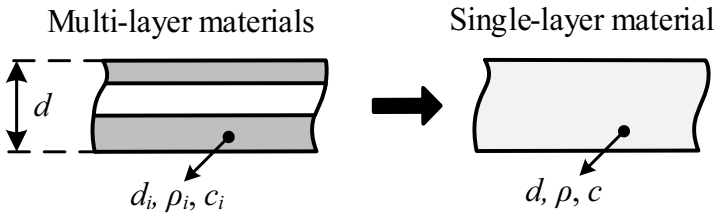

Fig. 1. The multi-layer materials are equivalent to single-layer material

Then, according to the law of conservation of mass and energy, the thermophysical parameters of the equivalent material [19] are derived, as shown in the formula below

$$\begin{cases} \rho = \left(\sum_{i=1}^{n} \rho_i d_i \right) \Big/ \sum_{i=1}^{n} d_i \\ \lambda = \left(\sum_{i=1}^{n} \lambda_i d_i \right) \Big/ \sum_{i=1}^{n} d_i \\ c = \left(\sum_{i=1}^{n} \rho_i c_i d_i \right) \Big/ \sum_{i=1}^{n} \rho_i d_i \end{cases} \tag{1}$$

where ρ, λ and c are the density, thermal conductivity and specific heat capacity of the equivalent material, respectively; ρ_i, λ_i, c_i and d_i are the density, thermal conductivity, specific heat capacity and thickness of the i-th-layer material, respectively, and n is the number of material layers.

After the multi-layer ultra-thin materials of the spherical wall are made equivalent to a single-layer material, the target heat transfer and temperature change can be calculated directly by using the parameters of Formula (1).

3 Theoretical Calculation Model for Point Target Temperature

3.1 Transient Temperature

When the space target is far away, it can be regarded as a point target, and its surface temperature is the same everywhere. For an inflatable sphere, at time t, the internal energy increase of the inflatable sphere is equal to the net energy absorbed at that time:

$$mc \frac{\mathrm{d}T(t)}{\mathrm{d}t} = Q_s + Q_e - \varepsilon_{out} \sigma T^4(t) S_0 \tag{2}$$

wherein m is the mass of the inflatable sphere, c is the specific heat capacity of equivalent material calculated with Formula (1), Q_s and Q_e are the energy absorbed by the target from the Sun and the Earth respectively, σ is Stefan-Boltzmann constant, the last term on the right side of Formula (2) is the radiation heat dissipation from the outer surface of inflatable sphere to the outer space, ε_{out} is the emissivity of the outer surface of inflatable sphere, and S_0 is the surface area of inflatable sphere. The above related variables can be expressed as:

$$\begin{cases} m = \rho\left(\pi R_0^2 d\right) \\ Q_s = \alpha_s E_0 \pi R_0^2 \\ Q_e = \left(\varepsilon_{out} E_e + \alpha_s E_r\right) \pi R_0^2 \\ S_0 = 4\pi R_0^2 \end{cases} \tag{3}$$

where ρ is the density of the equivalent material calculated by Formula (1), and d is the thickness of sphere wall; α_s is the average absorption rate of solar radiation on the inflatable sphere surface, E_0 is the solar constant, the value of which is taken as 1360W/m^2, and R_0 is the inflatable sphere radius; E_e is the radiation luminance of the Earth to the near-Earth space, the value of which is taken as 240W/m^2, and E_r is the energy of sunlight reflected by the Earth, the value of which is taken as $0.3E_0$ for the illuminated area, and as 0 for the shaded area of the Earth.

To find the change of inflatable sphere temperature with time, the differential equation of Formula (2) is converted into a backward difference equation, as shown in Formula (4):

$$mc\frac{T_{t+\Delta t}-T_t}{\Delta t}=Q_s+Q_e-\varepsilon_{out}\sigma T_{t+\Delta t}^4 S_0 \tag{4}$$

where Δt is the heat transfer time step size.

Let the initial temperature of the inflatable sphere be T_0, and substitute the m, Q_s, Q_e, and S_0 of Formula (3) into Formula (4), and then iteratively solve the transient temperature change of the inflatable sphere by the Gauss-Seidel method.

3.2 Steady-state Temperature

It is worth noting that when the heat dissipated by the external surface of the target is equal to the energy absorbed from the external heat source, the target temperature will reach an equilibrium state, namely:

$$Q_s+Q_e=\varepsilon_{out}\sigma T_\infty^4 S_0 \tag{5}$$

where, T_∞ is the target steady-state temperature. Substituting Formula (3) into Formula (5), according to the reference [12], we can get:

$$T_\infty=\left[\frac{\left(E_0+E_r\right)\dfrac{\alpha_s}{\varepsilon_{out}}+E_e}{4\sigma}\right]^4 \tag{6}$$

It can be seen from Formula (6) that when E_0, E_r and E_e remain unchanged, the equilibrium temperature of the inflatable sphere is only determined by the ratio of the average solar radiation absorptivity α_s of the outer surface and the emissivity ε_{out} of the outer surface.

4 Numerical Calculation Model for Target Temperature Distribution

4.1 Transient Temperature Distribution

Before obtaining the temperature distribution of the target, it is necessary to divide the target to obtain the micro-facets. According to the equivalent model of multilayer ultra-thin materials, for this method it is only needed to perform subdivision along zenith angle and azimuth angle, and then analyze the heating condition of the micro-facets. At time t, the heat transfer differential equation of the k-th micro-facet is:

$$m_k c\frac{\mathrm{d}T_k(t)}{\mathrm{d}t}=q_{kc}(t)+q_{ks}+q_{ke}+q_{kr}(t)-q_{kd}(t) \tag{7}$$

where, m_k is the mass of micro-facet, q_{kc} is the heat conduction between the micro-facet k and the surrounding micro-facets, q_{ks} and q_{ke} are the solar and Earth radiation energy absorbed by the outer surface of micro-facet k, q_{kr} is the radiation heat transfer energy absorbed by the inner surface of micro-facet k, and q_{kd} is the heat lost from the outer surface of micro-facet k to space.

Many references [12, 15, 19] have given the calculation methods of energy components. The differential equation of Formula (7) is transformed into a backward difference equation similar to Formula (4), and the initial temperature of the micro-facets is set. The transient temperature variation of each micro-facet can be iteratively solved by the Gauss-Seidel method, so that the transient temperature distribution of the inflatable sphere can be obtained.

4.2 Radiation Transfer Coefficient

It can be proved that when, due to the special properties of a sphere, the inner surface is a gray body, the radiation transfer coefficient between any two elements is always equal to its angular coefficient [20], which has nothing to do with the value of the emissivity ε_{in} of the inner surface.

As the inner surface of the inflatable sphere may be very smooth [12], at this time, any facet will produce specular reflection other than diffuse reflection on the radiation energy of other inner wall facets, so the gray approximation method cannot be used to calculate the radiation heat transfer term q_{kr} in Formula (7), but the Monte Carlo method should be preferred [21]. In this method, a large number of rays are generated at random positions and directions on the emission facets, then the collision position of each ray is tracked, and the reflection direction is calculated according to the reflection law. Because the reflected light only propagates in the spherical tangent circle, this characteristic can be used to find the coordinates of multiple reflection points of light rays at the same time [22], and calculate the absorbed energy of the facet to which the reflection point belongs according to the propagation attenuation model of light [23], so as to calculate the radiation transfer coefficient of the emission facet to all the inner facets.

The net radiation energy q_{kr} absorbed by the inner surface of the micro-facet k can be expressed as:

$$q_{kr}(t)=\sum_{i=1}^{N}F_{i-k}\varepsilon_{in}\sigma T_i^4(t)s_i-\varepsilon_{in}\sigma T_k^4(t)s_k \tag{8}$$

where $F_{i\text{-}k}$ is the radiation transfer coefficient from the inner surface of micro-facet i to the inner surface of micro-facet k, ε_{in} is the emissivity of the inner surface of the inflatable sphere, T_i is the temperature of micro-facet i, s_i is the area of the inner surface of micro-facet i, N is the number of micro-facets, T_k is the temperature of micro-facet k, and s_k is the area of the inner surface of micro-facet k.

4.3 Target Equivalent Radiation Temperature

Usually, the temperatures of the micro-facets of a space inflatable sphere target are different. Assuming that the equivalent radiation temperature of the entire target is T_{eq}, according to the law of conservation of energy:

$$\varepsilon_{out}\sigma T_{eq}^4(t)S_0=\sum_{k=1}^{N}\varepsilon_{out}\sigma T_k^4(t)s_k \tag{9}$$

where S_0 is the surface area of the inflatable sphere, s_k is the outer surface area of micro-facet k and T_k is the temperature of micro-facet k.

Then the target equivalent radiation temperature T_{eq} is:

$$T_{eq}(t)=\left[\frac{\sum_{k=1}^{N}s_kT_k^4(t)}{S_0}\right]^{\frac{1}{4}} \tag{10}$$

Comparing the calculated value of target equivalent radiation temperature of Formula (10) with the theoretical value of point target temperature change of Formula (4) the correctness of the numerical calculation model can be verified.

5 Results

5.1 Simulation Parameters

In this case, the material composition of the wall layer of the space inflatable sphere and the parameter setting refer to the data in reference [12]. The radius of the inflatable sphere R_0 equals 1.5m. The sphere wall consists of three layers of materials, which are aluminum, polyester and aluminum films from the

inside out. The thermophysical parameters of the materials are shown in Table 1. Table 2 shows the spectral parameters of three groups of inflatable spheres selected in this case.

Table 1. Parameters of the multi-layer sphere

Layer No.	Film material	Thickness d (m)	Density ρ (kg/m^3)	Specific heat c (J/kg/K)	Hest conduction coefficient λ (W/m/K)
Outer	Aluminum	2.54×10^{-6}	2700	904	230
Middle	Polyester	6.35×10^{-6}	1390	1150	0.1
Inner	Aluminum	2.54×10^{-6}	2700	904	230

Table 2. Spectral parameters of the outer surface

Group	Solar radiation absorption rate α_s	Self emissivity ε_{out}	$\alpha_s/\varepsilon_{out}$
1	0.192	0.036	5.33
2	0.54	0.45	1.20
3	0.19	0.94	0.20

As shown in Fig. 2, in the spherical coordinate system, the inflatable sphere is divided into 19 parts along the zenith angle direction ($\Delta\theta$ = 9.47°) and 40 parts along the azimuth direction ($\Delta\varphi$ = 9°). The zenith angle and azimuth angle of the Earth are (90°, -90°), and the zenith angle and azimuth angle of the Sun are (90°, 94.5°). The initial temperature of the inflatable sphere is 300K, and it remains stationary in space. Heat transfer time step Δt = 1s.

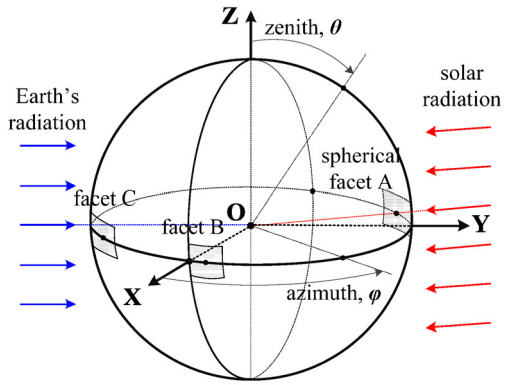

Fig. 2. Space Sphere Target and Simulation Scene

The calculation process of this paper is as follows:

1. For the outer surface spectral parameters of each group of inflatable spheres as shown in Table 2, first calculate the thermophysical parameters of equivalent material according to Formula (1), and then calculate the theoretical temperature variation curve and theoretical steady-state temperature of point targets according to Formula (4) and Formula (6) respectively.

2. For the outer surface spectral parameters of each group as shown in Table 2, when the inner surfaces of the inflatable spheres are in diffuse reflection or specular reflection (assuming ε_{in}=ε_{out}), calculate the radiation transfer coefficients between the facets respectively, so as to find the net radiation heat q_{kr} of Formula (8).

3. The transient temperature distribution of the inflatable sphere is calculated according to Formula (7), and the equivalent temperature change curve of the target is calculated according to Formula (10).

5.2 Equivalent Radiation Temperature

Fig. 3 shows the comparison between the theoretical value of point target temperature change calculated by Formula (4) and the target equivalent radiation temperature calculated by Formula (7) under the condition that the inflatable spheres have specularly-reflecting inner surface and diffusely-reflecting inner surface, respectively. Three cases are calculated and compared at $\alpha_s/\varepsilon_{out}$ = 0.20, 1.20 and 5.33 respectively.

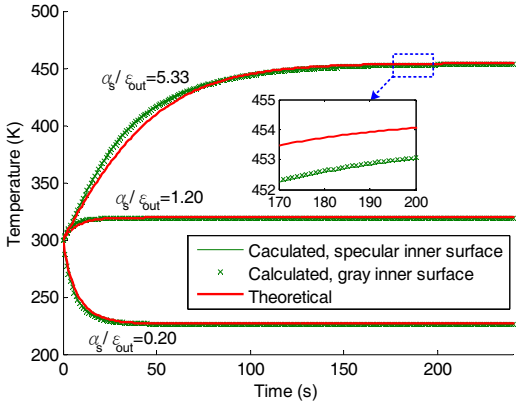

Fig. 3. Theoretical and calculated temperatures as a function of release time for point target

Table 3 shows the comparison between the theoretical value of point target equilibrium temperature calculated according to Formula (6) and the target equivalent radiation equilibrium temperature calculated according to Formula (10) when the values of $\alpha_s/\varepsilon_{out}$ are different.

Table 3. The theoretical and calculated equilibrium temperature of sphere in sunlight

Group	$\alpha_s/\varepsilon_{out}$	Theoretical value of equilibrium temperature (K)	Calculated value of equilibrium temperature (K)	
			Specular reflection	Diffuse reflection
1	5.33	454.4	453.6	453.6
2	1.20	319.4	318.9	318.9
3	0.20	226.5	226.2	226.2

5.3 Surface Temperature Distribution

Fig. 4 shows the target temperature distribution when $\alpha_s/\varepsilon_{out}$=5.33, ε_{in}=0.036 and t=300s, and the inner surfaces of the inflatable spheres are in specular reflection and diffuse reflection respectively. It can be seen from Table 3 that the overall equilibrium temperature of the target at this time is 454.4K, but due to the influence of solar and Earth radiation heating, the surface temperature difference of the target is significant. The facet A is directly facing the sun and has the highest temperature, while the facet B is not directly irradiated by external heat source and has the lowest temperature. Under the parameter settings in this paper, the maximum temperature difference between the inflatable sphere surfaces corresponding to the specularly-reflecting inner wall (Fig. 4(a)) and the diffusely reflecting inner wall (Fig. 4(b)) are about 171.5K and 157.3K, respectively, with a difference of 14.2K.

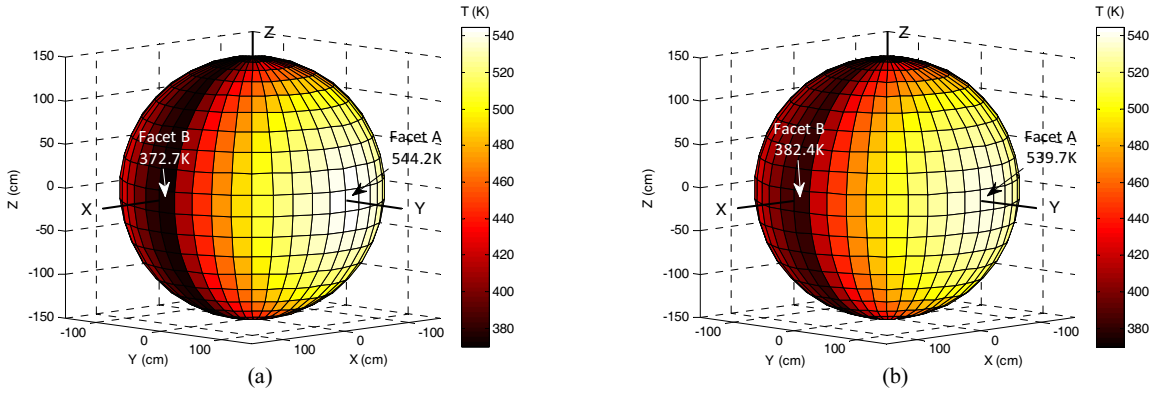

Fig. 4. Surface temperature of sphere with (a) specular and (b) gray inner surface at $\alpha_s/\varepsilon_{out}$=5.33, ε_{in}= 0.036

Fig. 5 shows the temperature distribution of the target surface when $\alpha_s/\varepsilon_{out}$=1.20, ε_{in}=0.45, and t=300s, and the inner surfaces of the inflatable spheres are in specular reflection and diffuse reflection

respectively. At this time, the maximum temperature difference between the inflatable sphere surfaces corresponding to the specularly-reflecting inner wall (Fig. 5(a)) and the diffusely-reflecting inner wall respectively (Fig. 5(b)) is about 109.4K, with a difference of 4.0K.

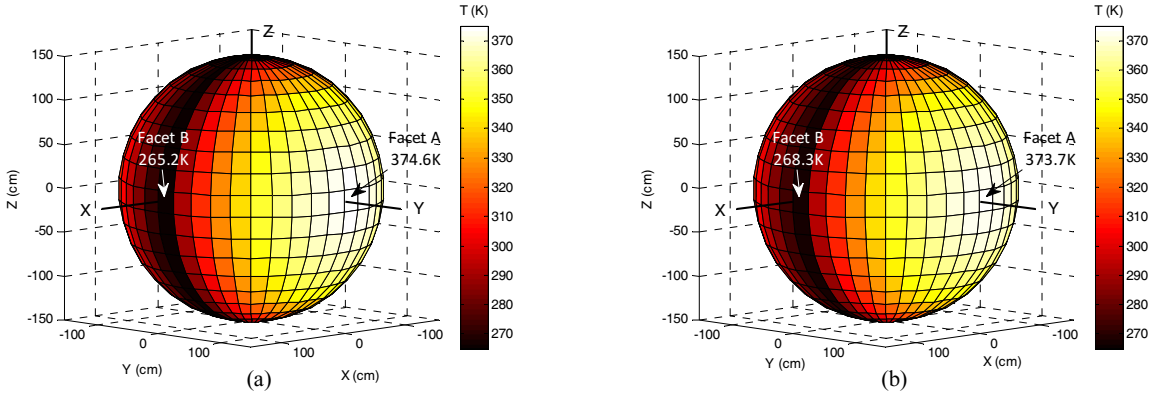

Fig. 5. Surface temperature of sphere with (a) specular and (b) gray inner surface at $\alpha_s/\varepsilon_{out}$=1.20, ε_{in}= 0.45

It can be seen from Fig. 6 that when $\alpha_s/\varepsilon_{out}$=0.20, ε_{in}=0.94, and t=300s, the temperature difference caused by the specularly-reflecting inner wall to the inflatable sphere surface is only 0.4K larger than that caused by the diffusely-reflecting inner wall, which is almost negligible.

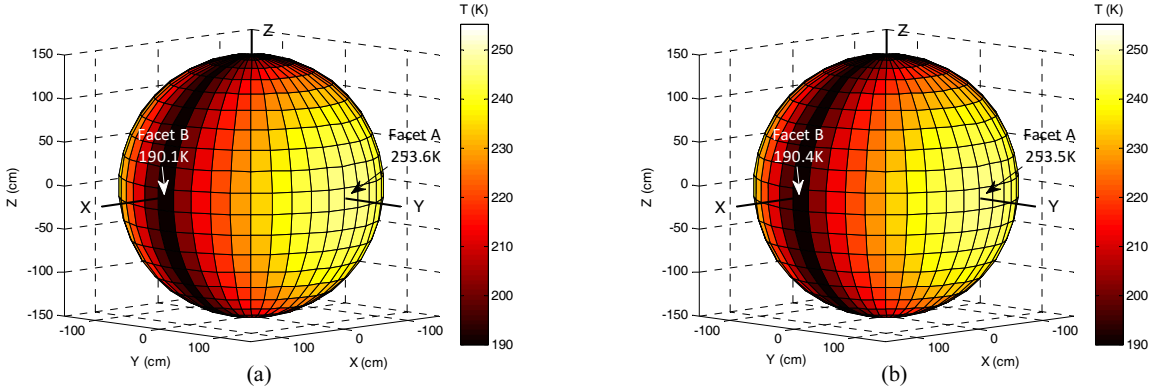

Fig. 6. Surface temperature of sphere with (a) specular and (b) gray inner surface at $\alpha_s/\varepsilon_{out}$=0.20, ε_{in}= 0.94

6 Analysis and Discussion

6.1 Theoretical and Calculated Temperature

Several results can be obtained from Fig. 3. First, theoretical temperature as a function of time indicates that different values of $\alpha_s/\varepsilon_{out}$ lead to different steady-state temperature. When $\alpha_s/\varepsilon_{out}$ is far less than 1.0, heat loss of the outer surface is greater than the solar heating, surface temperature of the point target will gradually decrease until the equilibrium temperature is reached. When $\alpha_s/\varepsilon_{out}$ is far less than 1.0, temperature will gradually rise to the equilibrium temperature. Formula (6) also confirmed that the steady-state temperature increases with the value of $\alpha_s/\varepsilon_{out}$.

Second, the calculated equivalent radiation temperature is in good agreement with the theoretical temperature for both specularly-reflecting and diffusely-reflecting inner surface cases. The calculation results shown in Fig. 3 also indicate that the reflection characteristics (diffuse reflection and specular reflection) of the inner surface of the inflatable sphere do not affect the equivalent radiation temperature of the target. As can be known from Formula (10), the equivalent radiation temperature of the object is calculated from the temperature of all the micro-elements. Different from the point temperature calculated in Section 3, the temperatures of these micro-elements are not the same, reflecting the temperature distribution on the target surface.

Third, surface temperature distribution is obtained by using the equivalent model of ultra-thin multilayer materials. Results in Fig. 3 proves the effectiveness of the equivalent model from one side. If the equivalent model is not used, the number of micro-elements of the ultra-thin multilayer target will become very large, making the calculation to be unable to proceed normally.

6.2 Surface Temperature Distribution

It can be seen from Fig. 4 to Fig. 6 that the surface temperature rises with the increasing of $\alpha_s/\varepsilon_{out}$, no matter what the reflection characteristic of the inner surface is. This is consistent with the results shown in Fig. 3. However, surface temperature distribution shows more detail than the equivalent radiation temperature. As can be seen from Fig. 4, at $\alpha_s/\varepsilon_{out}$=5.33, the highest temperature can reach up to over 500K and the lowest temperature is less than 400K for both specular and diffusing gray surface. However, surface temperature distribution is not the same when the characteristic of the inner surface is different, although the emissivity ε_{in} is the same for both cases.

As can be seen from Fig. 4 to Fig. 6, compared with diffuse reflection, the specular reflection characteristic of the inner surface makes the temperature difference on the inflatable sphere surface larger, especially when the emissivity ε_{in} of the inner surface is small. With the increase of ε_{in}, the influence of specular reflection on the superficial temperature difference gradually weakens, and the sphere's superficial temperature distribution in the case of specular reflection approaches that in the case of diffuse reflection.

The reason for this phenomenon is that the proportion of the radiation heat transfer allocated by each micro-element (i.e., the radiation heat transfer coefficient) is different for the specularly-reflecting inner surface and the diffusely-reflecting inner surface.

In order to quantify the radiative heat transfer energy absorbed by each micro-element on inner surface, the radiative heat transfer coefficients for all the inner surface micro-elements are calculated according to the Reference [20]. For each inner surface micro-element, the radiated energy will be absorbed eventually by all the micro-elements (including itself). The radiation transfer coefficient is the share of the energy finally absorbed by the receiving facet in the initial radiation energy of the emitting facet. Assuming there are N micro-elements, the radiation heat transfer coefficient matrix will be N*N. For simplicity, only the radiation heat transfer coefficient of micro-element A [central zenith angle 90°, azimuth angle 94.5°] is shown here to analyze the energy distribution.

Fig. 7(a) shows the radiation transfer coefficient matrix of emitting facet A [central zenith angle 90°, azimuth angle 94.5°] to all facets on the inner surface of the inflatable sphere when emissivity ε_{in}=0.036. It can be seen from Fig. 7(a) that, of the energy emitted by facet A, the share of the energy absorbed by facet A itself is 0.02225, and that absorbed by its spherically symmetric facet C [90°, 274.5°] is equivalent to it, which is much higher than that absorbed by facet A when the inner surface is gray, which is 0.002064, as shown in Fig. 7(d). It can be seen from Fig. 2 that as facet A is facing the Sun, the temperature is the highest, and the energy radiated to the spherical cavity is also the largest. In the case of specular reflection, the radiation energy of facet A is more distributed to itself, which leads to a higher facet temperature than in the case of diffuse reflection. Meanwhile, the more the energy absorbed by facet A, the less the energy absorbed by other facets, thus increasing superficial temperature difference.

It can be seen from Fig. 7(b-c) that with the increase of emissivity ε_{in}, the radiation heat transfer coefficient of facet A to itself gradually decreases. When ε_{in} is close to 1, as shown in Fig. 7(c), the radiation heat transfer coefficient of facet A to the overall facet is already very close to that of the inner surface with diffuse reflection as shown in Fig. 7(d), so the difference of surface temperature distribution between them is very small, as shown in Fig. 6. It is worth noting that the radiation transfer coefficients of the inner surface facets of an inflatable sphere are always equal to their respective angular coefficients during diffuse reflection.

On the other hand, during specular reflection, the phenomenon that the initial energy radiated by facet A into the spherical cavity is more absorbed by facet A itself is only established when the emissivity ε_{in} is low, while the low ε_{in} also makes the initial energy radiated by the facet A into the spherical cavity very low, limiting its potential of enlarging the surface temperature difference. This is also the reason why the temperature difference between the inflatable sphere with specularly-reflecting inner surface and that with diffusely-reflecting inner surface in Fig. 4 is not particularly significant under the parameter settings in this paper.

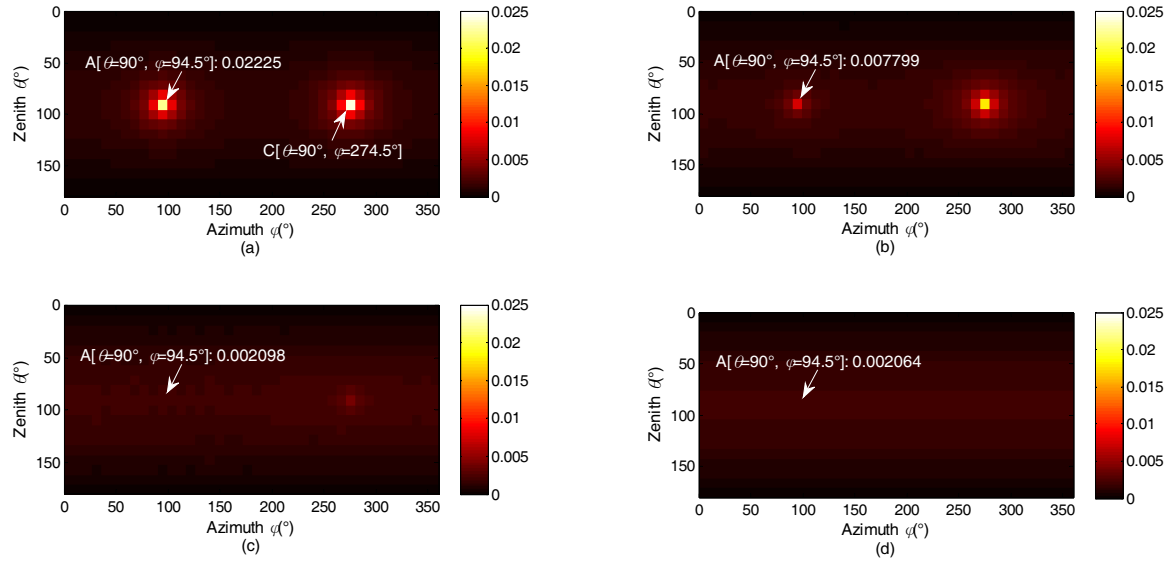

Fig. 7. Radiative heat transfer coefficient matrix between facet A [90°, 94.5°] and the whole spherical facet when specular inner surface emissivity ε_{in} is (a) 0.036, (b) 0.45, (c) 0.94 and (d) 1.00, respectively

6.3 Future Work

The paper discusses the influence of the inner surface reflection characteristics of the spherical target on the temperature distribution of the inflatable balloon. There is a lot of work to be further studied. Due to the particularity of the spherical target, its radiation heat transfer coefficient may have a certain particularity. Including the spherical balloon, space inflatable structures might have many other shapes, such as sphere-cone, etc. The influence of the inner surface reflection characteristics on the surface temperature of these objects requires further research.

7 Conclusion

In this paper, the equivalent model of ultra-thin multilayer materials is used to calculate the temperature distribution of inflatable sphere with time under the conditions of specular reflection and diffuse reflection. Results show that the calculated value of the target equivalent radiation temperature is consistent with the theoretical value of the point target temperature change, which validates the effectiveness of the material equivalent model. In addition, when the inner surface of the target is in specular reflection, the smaller the emissivity of the inner surface is, the greater the temperature difference of the target surface is due to the influence of the radiation transfer coefficient between the inner wall facets. When the emissivity increases, the surface temperature distribution is close to that of the diffusely-reflecting inner surface. Therefore, when the emissivity ε_{in} is large or the accuracy of temperature calculation is not particularly high, the radiation transfer coefficient (angle coefficient) of the diffusely-reflecting inner surface can be used to calculate the radiation heat transfer, so as to save the time of calculating the radiation transfer coefficient of specularly-reflecting inner surface by application of the Monte Carlo method.

Acknowledgements

This work is granted by Science and Technology Projects of Beijing Municipal Education Commission (KM201911232012), and Qin Xin Talents Cultivation Program, Beijing Information Science & Technology University (QXTCP C201905).

References

[1] J.-J. Yang, F.-F. Zhou, L.-S. Cui, J. Zhou, Infrared characteristics of ground targets and background observed from near space, Infrared Technology 43(7)(2021) 67-678.

[2] C.-Y. Wang, H.-Y. Zhao, X.-F. Li, C.-S. Liu, L.-G. Wang, J.-N. Wang, IR radiation imaging method of space target based on improved Delaunay triangulation, Laser & Infrared 50(2)(2020) 161-67.

[3] X. Li, J.-D. Li, H.-Z. Sun, L. Yang, Influencing factors of temperature and infrared characteristics of space target, Laser & Infrared 49(12)(2019) 1436-1441.

[4] W.-H. Li, C.-H. Liu, Y. Mu, D.-S. Liang, R. Yang, Modeling and research of infrared characteristics of space target based on radiation dissipation, Infrared and Laser Engineering 46(6)(2017) 0604003.

[5] F. Yang, Y.-M. Xuan, Y.-G. Han, Properties prediction of space objects based on infrared radiative characteristics, Scientia Sinica Technologica 46(8)(2016) 836-843.

[6] J.-L. Liu, Y.-F. Li, S.F. Chen, H.-Z. Lu, B.-D. Zhao, Micro-motion dynamics analysis of ballistic targets based on infrared detection, Journal of Systems Engineering and Electronics 28(3)(2017) 472-480.

[7] J. Zhang, H. Yang, Y.-S. Ling, Y.-S. Feng, Theoretical analysis of temperature field on the surface of ballistic missile warhead in midcourse, Infrared and Laser Engineering 34(5)(2005) 583-586.

[8] L.-X. Yao, Q.-P. Hou, J.-Q. Luo, Research on surface temperature and infrared signature of the ballistic warhead in midcourse, Aerospace Electronic Warefare 21(2)(2005) 5-16.

[9] H. X. Mao, H. Nan, J. Ma, Y.-B. Dong, K.-F. Wu, Analysis of influence of motion of attitude to optical character of space target, Infrared and Laser Engineering 36(s)(2007) 411-415.

[10] X.-A. Bai, Research on the effect of height on the radiation characteristics of spherical balloon decoy and missile, Infrared 41(6)(2020) 12-16.

[11] S.-D. Li, Research of releasing decoy outside atmosphere, Journal of Astronautics 22(2)(2001) 100-104.

[12] A.-M. Sessler, J.-M. Cornwall, B. Dietz, et al., Countermeasures: a technical evaluation of the operational effectiveness of the planned US national missile defense system, [report] Union of concerned scientists and MIT security studies program, 2000.

[13] X. Yang, X.-D. Wu, J. Chen, Differences of temperature distribution and infrared radiation feature between envelope balloon and spatial balloon, Infrared Technology 40(4)(2018) 395-399.

[14] S. Liu, X.-A. Zhu, F.-B. Li, Monte Carlo method for calculating radiative heat transfer coefficient of warhead envelope target, Tactical Missile Technology (3)(2018) 44-52.

[15] W.-T. Shen, D.-Q. Zhu, G.-B. Cai, Calculation of temperature field and infrared radiation characteristics of midcourse ballistic target, Journal of Astronautics 31(9)(2010) 2210-2217.

[16] M. Yang, Y.-L. Chu, Q. Chai, Warhead enveloping-ball and its application on penetration in infrared wavebands, Aerospace Electronic Warfare 25(4)(2009) 5-7, 20.

[17] G.-Q. Fang, K.-N. Teng, Modeling and simulation of target and background infrared image in middle trajectory of ballistic missile, Journal of Naval Aeronautical and Astronautical 28(6)(2013) 592-599.

[18] W.-Q. Zhang, Y.-M. Xuan, Y.-G. Han, A new method of radiative transfer coefficient between unit surfaces, Journal of Astronautics 26(1)(2005) 77-81.

[19] F.-B. Li, X.-J. Xu. Fast algorithm for temperature calculation of multi-layered ultra-thin decoy, Infrared and Laser Engineering 40(6)(2011) 986-991.

[20] F.-B. Li, H.-L. Li, Radiative heat transfer coefficient of the sphere target with gray inner surface, Natural Science Journal of Xiangtan University 39(2)(2017) 86-89.

[21] J.-R. Howell, M. Perlmutter, Monte Carlo solution of thermal transfer through radiant media between gray walls, Journal of Heat Transfer 86(1)(1964) 116-122.

[22] F.-B. Li, J.-M. Leng, H.-L. Li, Radiative heat transfer coefficient calculation of inflatable sphere with specular inner surface, Modern Defence Technology 45(3)(2017) 193-199, 214.

[23] D.-V. Walters, R.-O. Buckius, Monte Carlo methods for radiative heat transfer in scattering media, Annual Review of Heat Transfer (5)(1992) 131-176.